Fast-rate formation of TiO_2 nanotube arrays in an organic bath and their applications in photocatalysis

2010 Nanotechnology 21 365603

(http://iopscience.iop.org/0957-4484/21/36/365603)

Nanotechnology **21** (2010) 365603 (8pp) doi:10.1088/0957-4484/21/36/365603

Fast-rate formation of TiO_2 nanotube arrays in an organic bath and their applications in photocatalysis

Srimala Sreekantan[1,3], **Khairul Arifah Saharudin**[1], **Zainovia Lockman**[1] **and Teoh Wah Tzu**[2]

[1] School of Materials and Mineral Resources Engineering, University Sains Malaysia Engineering Campus, 14300 Nibong Tebal, Seberang Perai Selatan, Pulau Pinang, Malaysia
[2] Department of Civil and Environmental Engineering, Nagaoka University of Technology, 1603-1 Kamitomioka, Nagaoka, Niigata 940-2118, Japan

E-mail: srimala@eng.usm.my

Received 25 March 2010, in final form 26 July 2010
Published 13 August 2010
Online at stacks.iop.org/Nano/21/365603

Abstract

In this work, 18.5 μm titanium oxide (TiO_2) nanotube arrays were formed by the anodization of titanium (Ti) foil in ethylene glycol containing 1 wt% water and 5 wt% fluoride for 60 min at 60 V. The fast growth rate of the nanotube arrays at 308 nm min^{-1} was achieved due to the excess fluoride content and the limited amount of water in ethylene glycol used for anodization. Limited water content and excess fluoride in ethylene glycol inhibited the formation of a thick barrier layer by increasing the dissolution rate at the bottom of the nanotubes. This eased the transport of titanium, fluorine and oxygen ions, and allowed the nanotubes to grow deep into the titanium foil. At the same time, the neutral condition offered a protective environment along the tube wall and pore mouth, which minimized lateral and top dissolution. Results from x-ray photoelectron spectra revealed that the TiO_2 nanotubes prepared in ethylene glycol contained Ti, oxygen (O) and carbon (C) after annealing. The photocatalytic activity of the nanotube arrays produced was evaluated by monitoring the degradation of methyl orange. Results indicate that a nanotube with an average diameter of 140 nm and an optimal tube length of 18.5 μm with a thin tube wall (20 nm) is the optimum structure required to achieve high photocatalytic reaction. In addition, the existence of carbon, high degree of anatase crystallinity, smooth wall and absence of fluorine enhanced the photocatalytic activity of the sample.

1. Introduction

Titanium dioxide (TiO_2) is a semiconductor material that has been studied extensively in the last few decades due to its chemical stability, nontoxicity and high photocatalytic activity [1]. It has been used to eliminate pollutants, as a gas sensor, an electrode in solar cells and a catalyst support. Due to its photocatalytic activity, TiO_2 has also been used as a photocatalyst in the degradation of organic compounds that pollute the environment [1]. Owing to the one-dimensional (1D) nature of TiO_2 nanotubes, which offer a high surface area for photocatalytic reaction, they provide better performance compared to nanoparticles. Therefore, numerous fabrication methods, such as electrochemical lithography [2], photoelectrochemical etching [3], sol–gel processing [4], hydrothermal synthesis [5] and template synthesis [6, 7], have been used to form nanotubes and other 1D TiO_2 structures (e.g. nanowires, nanodots and nanorods). Among these processes, electrochemical anodization of titanium in fluorinated electrolytes is a relatively simple method to synthesize porous or tubular structures. Gong *et al* [8] were the first to report on the formation of TiO_2 nanotubes using an acidified fluoride aqueous electrolyte under anodic oxidation. For successful TiO_2 formation, the acidified fluoride solution must have a pH less than 5. However, under this condition, oxide dissolution rate is high and only a limited length (500 nm) of nanotube can be produced. Cai *et al* [9] used a range of pH for the electrolyte to reduce the dissolution

[3] Author to whom any correspondence should be addressed.

Table 1. Formation rate of TiO_2 nanotubes produced in various electrolytes. (Note: EG = ethylene glycol.)

Anodization condition	Tube length (μm)	Rate of formation (nm min^{-1})
EG, 60 V, 0.3 wt% NH_4F, 2% H_2O, 5760 min [11]	380	66.0
EG, 60 V, 0.4 wt% NH_4F, 2.5% H_2O, 10 080 min [11]	538	53.3
EG, 60 V, 0.5 wt% NH_4F, 3% H_2O, 12 960 min [11]	1000	76.7
DMSO, 60 V, 2 wt% HF, 4200 min [11]	101	23.3
EG, 60 V, 0.25 wt% NH_4F, 1% H_2O, 1020 min [12]	139	136.3
EG, 60 V, 0.3 wt% NH_4F, 2% H_2O, 1020 min [12]	220	215.6
EG, 60 V, 0.25 wt% NH_4F, 2% H_2O, 240 min [13]	22	91.7
EG, 60 V, 0.5 wt% HF, 10% H_2O, 1440 min [1]	15	10.4
EG, 60 V, 5 wt% NH_4F, 60 min (current work)	5	83.3
EG, 60 V, 5 wt% NH_4F, 1.0% H_2O, 60 min (current work)	18.5	308.3

rate of the oxide. Nanotubes of about 6 μm were achieved under such conditions. Recently, we have shown that the use of a neutral bath can obtain up to 3 μm nanotubes, provided that excess fluoride exists in the bath [10]. However, one of the major drawbacks of using an aqueous-based electrolyte is the slow growth of nanotubes. This drawback can be overcome with the use of an organic solvent. Paulose *et al* [11] introduced the use of organic electrolytes, such as ethylene glycol (EG), formamide (FA), dimethyl sulfoxide (DMSO) and dimethylformamide (DMF), for the formation of nanotubes ranging from 10 to 1000 μm in length. In their work, the highest growth rate achieved was 76.7 nm min^{-1} (table 1). However, these experiments are difficult to adopt in a robust industrial production setting because of the required lengthy process of anodization. Table 1 shows a summary of the studies conducted by a few authors on the formation of TiO_2 nanotubes in an organic electrolyte. The conditions adopted for this work are also presented. In this present work, TiO_2 nanotube arrays were formed in glycerol and ethylene glycol containing 5 wt% NH_4F. The aim was to produce high aspect ratio nanotubes in the shortest anodization time possible. A growth rate as high as 308.3 nm min^{-1} was achieved using ethylene glycol with excess fluoride and limited water content. The findings of the present study are summarized in table 1. Additionally, a discussion on the fast-rate formation of nanotubes is presented in subsequent sections.

2. Experimental procedure

Titanium foils (0.1277 mm thickness, 99.6% purity) were purchased from STREM Chemicals. Anodization was performed in a standard two-electrode bath with Ti foil as the working electrode and platinum as the counter electrode. Prior to anodization, the Ti foil was sonicated in ethanol for 15 min, rinsed with deionized water and then air-dried. After drying, the foil was exposed to an electrolyte consisting of either glycerol or ethylene glycol. The solutions were used as purchased without any purification. Next, 5 wt% NH_4F was added. The purity of the glycerol is 85% (with 15% water) while that of ethylene glycol is 100%. Anodization voltage was 20 V for the sample prepared in glycerol while 30 and 60 V were used for samples prepared in ethylene glycol. The conditions are chosen based on our preliminary studies which indicated that TiO_2 nanotubes can be produced when the voltage is maintained around this value. Finally, the anodized Ti foil was sonicated in distilled water for 30 s.

The morphologies of the anodized Ti were characterized by a field emission scanning electron microscope (FESEM) SUPRA 35VP Zeiss operating at a working distance of 4 mm with an accelerating voltage of 5 kV. To obtain the thickness of the formed anodic layer, a cross-sectional measurement was performed on mechanically bent samples. The actual length of the nanotubes was estimated by dividing the length on the micrograph by cos 45°. Chemical stoichiometry of the sample was investigated using energy dispersive x-ray (EDX) analysis. The crystal phases of the TiO_2 nanotubes were studied by x-ray diffraction (XRD) using the Philips model PW 1729, which was operated at 45 kV and 40 mV. Fluorescence spectra were recorded at room temperature using an LS 55 luminescence spectrometer (Jobin-Yvon HR). Chemical states were characterized by x-ray photoelectron spectroscopy (XPS) (JEOL JPS-1000SX) with an Mg Kα x-ray source. Photocatalytic degradation studies were performed by dipping a piece of 3 cm^2 Ti foil in 100 ml 30 ppm methyl orange (MO) in a customized photoreactor made of quartz glass. The sample was left in the reactor for 30 min in a dark environment to achieve adsorption/desorption equilibrium. It was photoirradiated at room temperature using TUV 18 W UV-C germicidal light, and then 5 ml solution was withdrawn every 1 h from the quartz tube to monitor the degradation of methyl orange after irradiation. The concentration of the degraded methyl orange was determined using a UV spectrometer.

3. Results and discussion

3.1. Anodization of titanium in glycerol

Electrochemical anodization was performed in 100 ml glycerol with the addition of 5 wt% NH_4F at 20 V for 60 min. The condition was chosen based on our preliminary studies, which favored the formation of well-aligned TiO_2 nanotube arrays [14]. As shown in figures 1(a) and (b), the anodized titanium consisted of a nanotubular oxide with a regular and clear pore structure. The pore diameters averaged 90 nm and the length of the nanotubes was about 0.8 μm. The inset in figure 1(b) shows the bottom part of the nanotubes. The so-called barrier layer has a dome-like shape. The pores are, however, not exactly circular and the ridges on the circumference of the nanotubes are obvious. This finding is

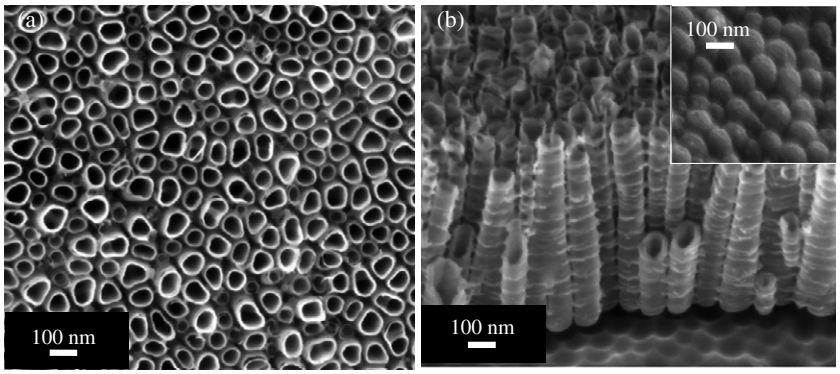

Figure 1. FESEM images of TiO_2 nanotubes formed in glycerol at 20 V for 60 min.

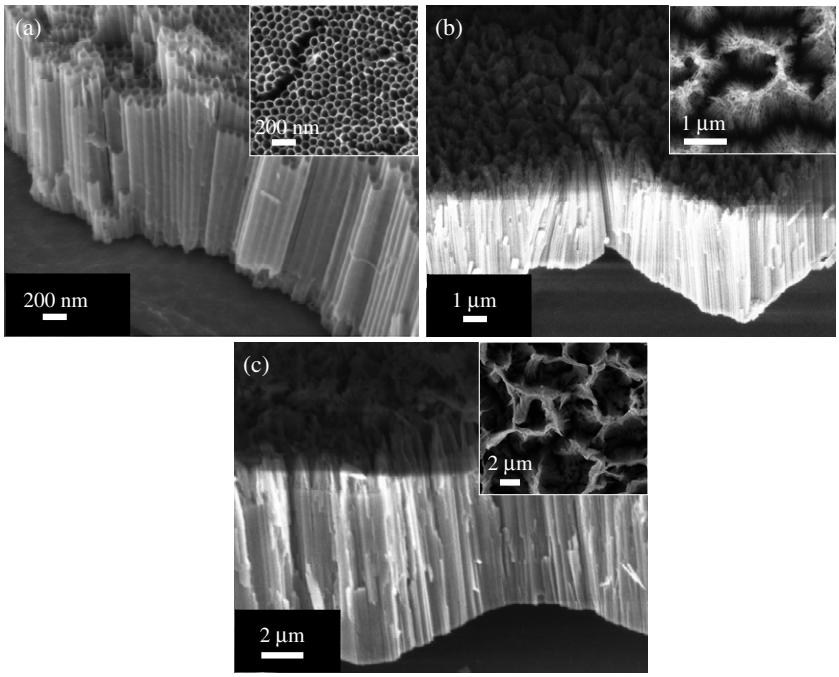

Figure 2. FESEM images of TiO_2 nanotubes formed at different anodization times in ethylene glycol electrolyte with 5 wt% NH_4F at 30 V: (a) 60 min, (b) 180 min and (c) 360 min.

different compared to the reported work by Schmuki, who claimed the formation of nanotubes with a smooth surface in glycerol [15]. The difference might be due to the existing water (15 wt%) in the glycerol, which caused a pH burst, and thus made the surface of the nanotubes serrated.

3.2. Anodization of titanium in ethylene glycol

The next set of experiments was carried out using ethylene glycol with 5 wt% fluoride. The anodization voltage was kept constant at 30 V and three anodization times (60, 180 and 360 min) were investigated. The growth rate of the nanotubes is expected to be high in ethylene glycol because it is less viscous ($\eta = 16$ cP at 25 °C) compared to glycerol ($\eta = 945$ cP at 25 °C). This translates to longer nanotubes in ethylene glycol [16]. Figures 2(a)–(c) show the FESEM images of anodized titanium foils at 60, 180 and 360 min, respectively. As shown in figure 2(a), the use of ethylene glycol allows for the formation of nanotube arrays. The diameters of the nanotubes are more uniform and the nanotube walls are smoother. The length of the nanotubes after 60 min was 1.7 μm with a formation rate of 28.3 nm min^{-1}. Prolonging the anodization time to 180 min and 360 min resulted in longer nanotubes with lengths of 5 μm and 13.7 μm, respectively. Nanotubes produced at long times seemed to accumulate and form a cone-like structure until the oxide layer at their top sections collapsed. Nanotube formation in a fluoride-containing organic electrolyte has been elaborated by Prakasam [17]. From here, it is clear that the slow rate of nanotube formation can be attributed to the insufficient anodic current flow, which is required to enhance electrochemical dissolution of Ti metal ions in ethylene glycol, as well as to induce field-assisted oxidation of Ti metal to form TiO_2.

One way to improve field-assisted dissolution is to increase the anodization voltage. In this set of experiments, anodization voltage was increased to 60 V while time was

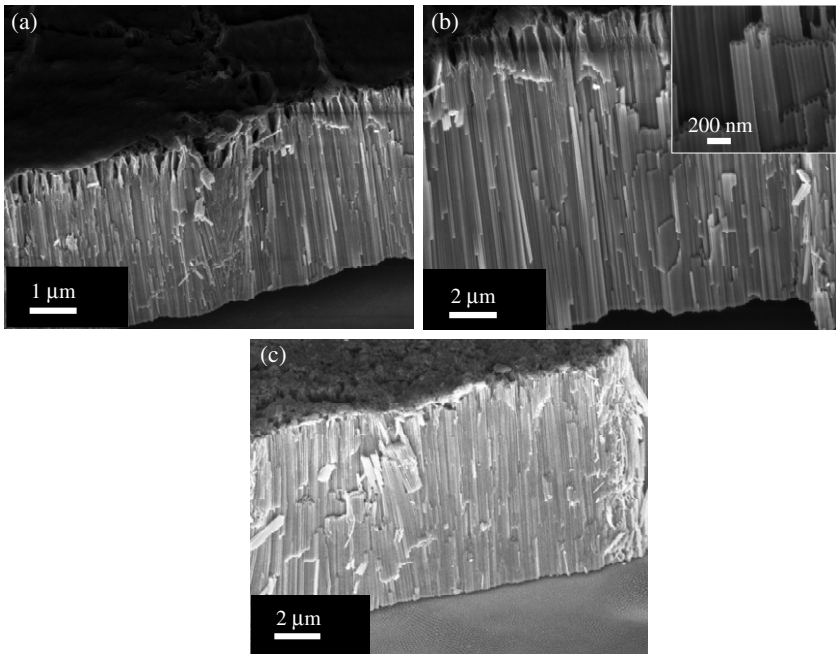

Figure 3. FESEM images of TiO_2 nanotubes formed in ethylene glycol electrolyte at 60 V with different amount of water added: (a) 0 wt%, (b) 1 wt% and (c) 2 wt%.

kept constant at 60 min. As shown in the FESEM image in figure 3(a), TiO_2 nanotubes with an average length of 5 μm were produced after 60 min of anodization, indicating the enhancement of electrochemical dissolution and the oxidation of Ti at 60 V. The rate of formation is approximated at 83.3 nm min^{-1}. It is anticipated that the addition of water in ethylene glycol will increase the rate of nanotube formation [13]. Therefore, another set of experiments was carried out to investigate the effect of water. Longer nanotubes with a length of 18.5 μm (figure 3(b)) were produced when 1 wt% water was added to ethylene glycol. The calculated rate of formation was approximately 308 nm min^{-1}, much higher compared to values reported so far in the literature (table 1). The fast rate of formation in this work is mainly attributed to the degree of dissolution of the anodic oxide, which was controlled by two factors: pH and fluoride content. These factors will be discussed in detail in succeeding sections. If water content is increased further to 2 wt%, the nanotubes become short (13 μm), as shown in figure 3(c).

During anodization, the dissolution of TiO_2 occurs at both the top (oxide electrolyte interface) and the bottom (inside the channel) of the nanotubes. To increase the rate of formation, reducing the dissolution at the top of the nanotubes while ensuring continual dissolution inside the nanotubes at the barrier layer is necessary. By maintaining the electrolyte at neutral condition, the dissolution at the top can be suppressed. To ensure continual dissolution at the bottom of the nanotubes, two processes can be controlled: the rate of anodic oxidation and the rate of chemical dissolution (figure 4). Inside the nanotubes, chemical dissolution may occur due to H^+ and F^- ions. As seen in equation (1), whenever oxidation occurs, H^+ is released; this is followed by an increase in local acidification at the bottom of the nanotubes. Local acidification

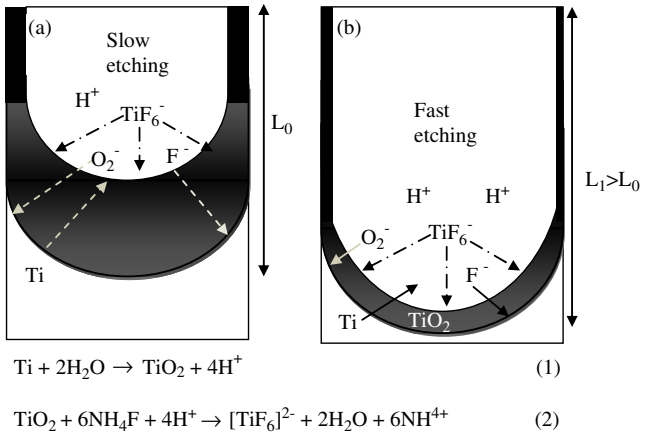

$$Ti + 2H_2O \rightarrow TiO_2 + 4H^+ \quad (1)$$

$$TiO_2 + 6NH_4F + 4H^+ \rightarrow [TiF_6]^{2-} + 2H_2O + 6NH^{4+} \quad (2)$$

Figure 4. Schematic diagram illustrating the thinning procedure of the oxides at the bottom of the nanotubes: (a) less fluoride results in a thick oxide layer which suppresses the transport of titanium, oxygen and fluorine ions, and (b) excess fluoride results in a thin oxide layer which enhances the transport of titanium, oxygen and fluorine ions, thus inducing inward growth faster (L_1 and L_o represent the lengths of the tubes in each aforementioned condition).

in the nanotubes accelerates the chemical dissolution process in accordance with equation (2). As seen in the equation, the formation of the nanotubes is related to the diffusion of F^- ions through the oxide layer and effusion of $[TiF_6]^{2-}$. Therefore, the high rate of formation of TiO_2 nanotubes in this work can be explained by the presence of excess amounts of F^- content, the value of which is needed to accelerate equation (2). The accelerated rate of etching thinned the barrier layer, which induced a faster inward growth (figure 4(b)). The higher the content of F^-, the faster the rate of etching of the oxide

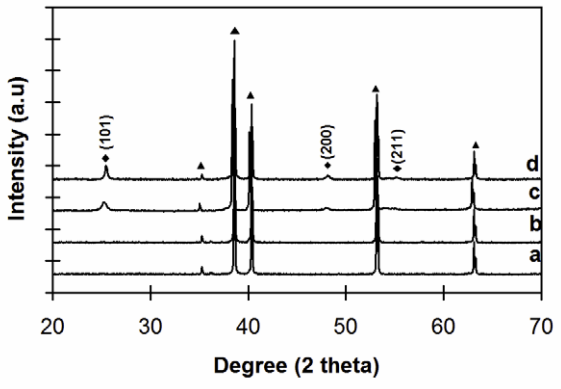

Figure 5. XRD patterns of titanium: (a) anodized in glycerol and not annealed, (b) anodized in ethylene glycol and not annealed, (c) anodized in glycerol and annealed at 400 °C in argon and (d) anodized in ethylene glycol and annealed at 400 °C in argon. (▲: Ti, ♦: anatase).

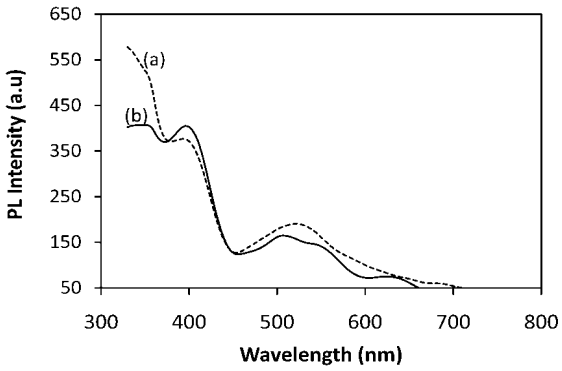

Figure 6. Photoluminescence spectra of TiO_2 nanotubes anodized in (a) ethylene glycol and annealed at 400 °C in argon and (b) glycerol and annealed at 400 °C in argon.

layer. When the oxide layer is thin enough, the transport of titanium and oxygen ions occurs easily and assists further in the anodic oxidation reaction. Nevertheless, in ethylene glycol, the donation of oxygen is more difficult compared to an acidified solution, thus reducing the tendency to form a thick oxide at the bottom of the nanotubes. In the present study, the amount of added water is also very important. As mentioned, in ethylene glycol, the availability of oxygen ions needed for oxidation is less. When water is used, the water molecules could ensure the oxidation process proceeds easily.

3.3. Effects of heat treatment

It has been well documented that as-made TiO_2 nanotubes are amorphous [14]. To investigate the effects of heat treatment on the crystal structure of the sample prepared in glycerol, ethylene glycol heat treatment was employed at 400 °C. The crystalline structure was examined using XRD. Heat treating the nanotubes at 400 °C is expected to result in an anatase phase, hence the nanotubes would present excellent photocatalytic activity [14]. Figure 5 shows the XRD patterns of the as-anodized sample and those after heat treatment. Evidently, the as-anodized sample was amorphous; only Ti peaks were seen. Samples annealed at 400 °C were crystalline with anatase TiO_2. Although the dominant structure of the sample annealed at 400 °C is anatase, the peak intensity of the (101) plane of the sample made in ethylene glycol is stronger than that of the sample made in glycerol. This implies that samples made in ethylene glycol have better crystallization than samples made in glycerol.

3.4. Photoluminance

The photoluminance (PL) technique has been widely used to investigate the energy levels of materials. The room temperature PL spectra of TiO_2 nanotubes annealed in argon were obtained using an excitation wavelength of 325 nm in the range of 350–600 nm. Typically, the TiO_2 nanotube PL spectra are composed of UV emission and a visible emission band (figure 6). The emission for the sample made in ethylene glycol was positioned at 350 (3.66 eV), 400 (3.0 eV) and 527 nm (2.3 eV), while the sample made in glycerol was located at 350 (3.66 eV), 400 (3.0 eV) and 504 nm (2.5 eV). A similar value of UV emission at 3.66 and 3.0 eV for both samples indicates the probability of band-to-band recombination (i.e. intrinsic states rather than surface states). Similar findings were reported by Daude *et al* [18], whereby the PL bands at 3.66 and 3.0 eV can be assigned to the highest energy direct transition and lowest energy indirect transition, respectively. On the other hand, the visible light emission at 2.3 and 2.5 eV were very close to the shallow trap level, which may be attributable to the oxygen vacancies giving rise to donor states located below the conduction band. The values reported in this work are consistent with those reported by Liqiang *et al* [19], Withana and Micha [20] and Shi *et al* [21].

3.5. Chemical composition

Figures 7(a)–(d) show the high-resolution C 1s, Ti 2p, O 1s and F 1s XPS spectra of the sample anodized in ethylene glycol and glycerol. The Ti 2p spectra of the TiO_2 nanotubes are shown in figure 7(a). In addition to the two characteristic peaks of Ti $2p_{1/2}$ at 465 eV and Ti $2p_{3/2}$ at 459.2 eV, another additional peak was present at 450.8 eV. According to the literature [13], the peak at 450.8 eV can be assigned to Ti, which may have originated from the substrate because of fractures in the oxide layer. The C 1s spectra for TiO_2 made in ethylene glycol and glycerol were similar and revealed two peaks at 284.9 and 289.0 eV as well as an additional shoulder at 286.5 eV (figure 7(b)). The strong peak positioned at 284.9 eV is usually assigned to adventitious elemental carbon, which cannot be eliminated. This peak also existed in the case of the pure TiO_2 sample [22] and it was close to the position of graphitic sp^2-hybridized carbon (284.9 eV) [23]. The peak at 286.5 eV could be ascribed to Ti–C–O bonds that comprise the carbonate species. This happens when C atoms are incorporated into the interstitial positions of the TiO_2 lattice [24, 25] during pyrogenation of the organic compound [22]. Meanwhile, the weak peak at 289.0 eV indicated that a small amount of carbonate species was present on the surface [26, 5, 27].

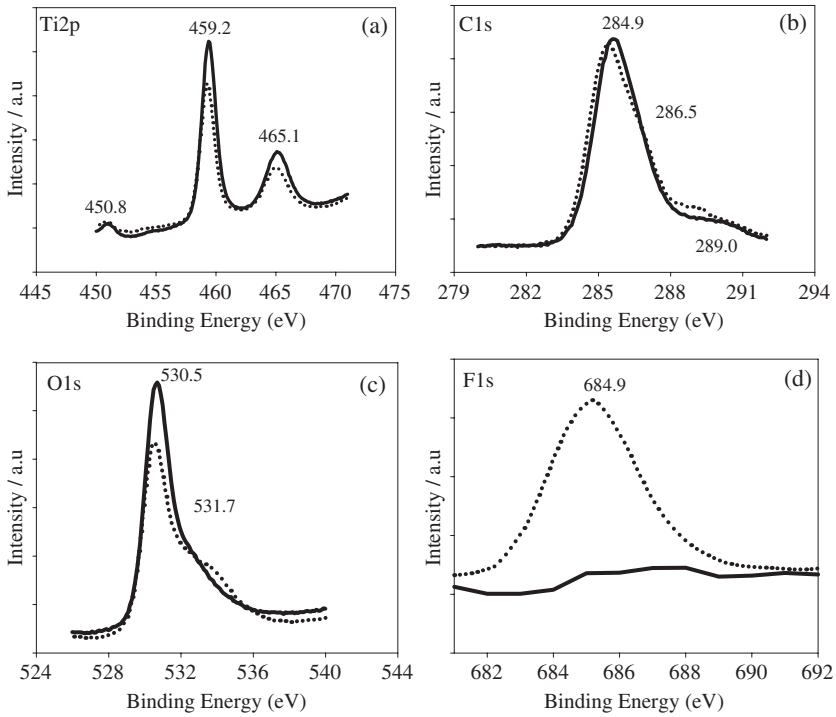

Figure 7. XPS high-resolution spectrum of the surfaces: (a) Ti 2p, (b) C 1s, (c) O 1s and (d) F 1s. (Solid line: TiO_2 nanotubes formed in ethylene glycol and annealed at 400 °C in argon; dotted line: TiO_2 nanotubes formed in glycerol and annealed at 400 °C in argon.)

Table 2. Experimental condition to obtain tubes 140 nm in diameter with different lengths.

Nanotube length (μm)	Electrolyte	Anodization condition
2.6	Ethylene glycol + 5 wt% F^-	pH 7, 60 V, $t = 30$ min
5	Ethylene glycol + 5 wt% F^-	pH 7, 60 V, $t = 60$ min
18.5	Ethylene glycol + 5 wt% F^- + 1 wt% H_2O	pH 7, 60 V, $t = 60$ min

No peak occurred at around 281 eV, which represents Ti–C bonds, for the two samples (made in ethylene glycol and glycerol). This suggests that carbon did not substitute for oxygen atoms in the lattice of TiO_2, which usually results in the formation of O–Ti–C [28, 29]. Because the XRD pattern also did not indicate the formation of Ti–C bonds, Ti–C–O bonds most likely formed. The O 1s spectra (figure 7(c)) showed a sharp peak at 530.0 eV, which is associated with TiO_2, and a shoulder at 531.7 eV. The additional shoulder could be related to the presence of organic compounds with C–O or C=O bonds [13]. Figure 7(d) shows the F 1s spectra. One peak existed at 684.9 eV for TiO_2 made in glycerol and none for the sample made in ethylene glycol. The peak positioned at 684.9 eV could be related to Ti–F-type compounds, possibly $(NH_4)_2TiF_6$ [30, 31]. Overall, the XPS results, especially the C 1s XPS spectra, strongly suggested that the anodization of Ti in ethylene glycol and glycerol likely resulted in the introduction of carbon to the crystal structure of TiO_2. It is also worth noting that the sample made in ethylene glycol was free from fluoride content.

3.6. Photocatalytic activity

The photocatalytic activity of anodized TiO_2 nanotubes with a different surface structure was evaluated in the photodegradation of MO under UV light irradiation. To evaluate the effect of nanotube length on its photocatalytic activity, the degradation of MO was carried out with nanotubes that had a similar diameter (140 nm) but different lengths (∼2.6, 5 and 18.5 μm). The experimental condition used to achieve such tubes is summarized in table 2.

As shown in figure 8, TiO_2 nanotubes with a length of 2.6 μm exhibited a lower degree of MO degradation (70%), followed by nanotubes with a length of 5 μm (85%) and 18.5 μm (90%). The increase in photocatalytic activity for the longer nanotubes may be attributed to their large surface areas, which led to better diffusion of reactant inside the nanotubes. However, beyond 5 μm, there was not much enhancement in photocatalytic activity. This result is in good agreement with the result reported by Liang *et al* [32]; in the report, if the nanotube length is longer than the effective depth of light penetration, there is difficulty for the lower part to absorb light. This suggests that the photocatalytic activity cannot be improved when the nanotube length exceeds a certain range because of the limited amount of absorbed incident photons.

Figure 9 shows the photocatalytic activity of TiO_2 nanotubes prepared in aqueous solution, glycerol and ethylene glycol. The experimental condition used to achieve such tubes is summarized in table 3. The TiO_2 nanotubes prepared

Table 3. Experimental condition and the corresponding EDX elemental analysis of TiO_2 nanotubes with 90 nm diameter and 0.8 μm length produced in aqueous solution, ethylene glycol and glycerol.

		EDX analysis (at.%)			
Electrolyte	Anodization condition	Ti	O	C	F
Aqueous solution (1 M Na_2SO_4) + 3 wt% F	pH 4, 20 V, $t = 60$ min	47.37	52.63	—	—
Glycerol + 5 wt% F	pH 7, 20 V, $t = 60$ min	64.17	31.13	3.84	1.86
Ethylene glycol + 5 wt% F	pH 7, 30 V, $t = 30$ min	60.31	35.11	5.58	—

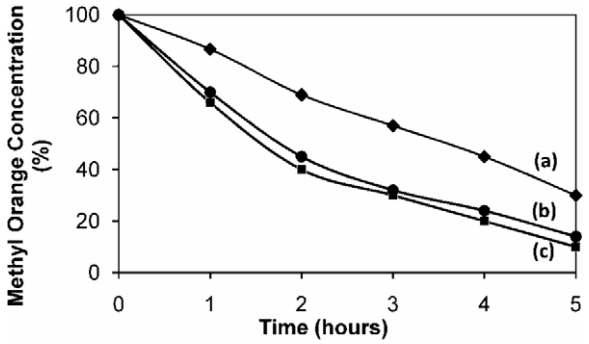

Figure 8. The photodegradation of MO using TiO_2 nanotubes with different lengths: (a) 2.6 μm, (b) 5 μm and (c) 18.5 μm.

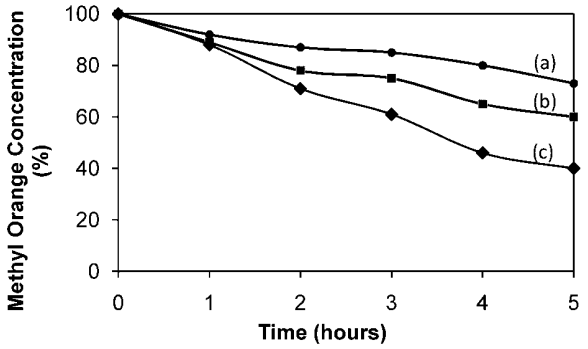

Figure 9. Photodegradation of MO using TiO_2 nanotubes produced in three different electrolytes: (a) aqueous solution (Na_2SO_4), (b) glycerol and (c) ethylene glycol.

in ethylene glycol produced the greatest degradation, which was 40% faster than that of TiO_2 nanotubes prepared in an aqueous solution. The TiO_2 nanotubes made in glycerol were 17% better than those made in aqueous solution. Because the wall thickness, diameter, length and crystal structure of all three samples were almost similar (thickness: 20 nm; diameter: 90 nm; length: 800 nm; crystal structure: anatase) it is believed that the greater degradation by TiO_2 nanotubes made in glycerol and ethylene glycol is due to carbon doping. Based on the EDX elemental analysis (not shown), the carbon content of the sample anodized in aqueous solution was 0 at.%, whereas the sample prepared in glycerol and ethylene glycol had a carbon content of 3.84 and 5.58 at.%, respectively. XPS results further supported the presence of carbon in TiO_2 crystal structures prepared in glycerol and ethylene glycol. Enhancement of MO degradation with carbon doping may be further explained on the basis of the bandgap energy of TiO_2. Because the bandgap is reduced by oxygen vacancies, photogenerated electrons and holes gain extra energy to reach the conduction and valence band, respectively, and carbon acts as an inhibitor for the electron–hole recombination. This leads to the formation of more oxidation radicals, resulting in better degradation of the reactants. Comparing TiO_2 prepared in glycerol and ethylene glycol, nanotubes prepared in ethylene glycol exhibited a higher degradation. The high degree of crystallinity, smooth wall and the absence of fluoride species are believed to be responsible for the enhancement of photoactivity of the TiO_2 nanotubes prepared in ethylene glycol. With regard to the smoothness of the wall, ridges on the circumference of the nanotubes produced in glycerol might have resulted in a light scattering point. This limited the amount of light penetrating to the bottom of the nanotubes, leading to poor degradation. In contrast, the smooth wall of TiO_2 nanotubes made in ethylene glycol enhanced light penetration, resulting in higher photodegradation. The XRD analysis showed that samples made in ethylene glycol had better crystallization of the anatase phase than samples made in glycerol, resulting in enhanced photodegradation. Furthermore, XPS results showed that TiO_2 prepared in ethylene glycol was free from fluoride content, but this was not the case for glycerol. Fluoride was detrimental to MO photodegradation because it exchanged with the hydroxyl groups at the TiO_2 surface. The hydroxyl group was essential to increase the overall efficiency of the MO degradation reaction [33].

4. Conclusions

We have investigated the formation of well-aligned nanotubes in fluorinated glycerol and ethylene glycol electrolytes. Long tubes with a smooth surface and a regular structure were obtained in ethylene glycol. In contrast, short tubes with a very rough and irregular structure were obtained in glycerol. In ethylene glycol, nanotubes can be grown up to 18.5 μm under optimized conditions of a voltage of 60 V, fluoride content of 5 wt%, water content of 1 wt% and anodization time of 60 min. The well-aligned layers are amorphous in nature, which can be transformed into anatase upon annealing at 400 °C. Based on the photocatalytic results, anodic TiO_2 with a length of 18.5 μm was deemed efficient for MO degradation. At the same time, photocatalytic activity was not significantly enhanced when the tube length exceeded 5 μm. Based on this study, we inferred that, other than the TiO_2 nanotube morphology and structure, other factors (e.g. oxygen vacancies, degree of crystallinity, wall texture, and presence of carbon and fluoride) also play important roles in determining the photocatalytic activity of TiO_2 nanotubes.

Acknowledgments

The authors would like to thank University Sains Malaysia Research University grant no. 811073, USM-RU-PGRS grant no. 8043045 and USM Fellowship for sponsoring this work.

References

[1] Mohapatra S K, Misra M, Mahajan V K and Raja K S 2007 *J. Phys. Chem.* C **111** 8677–85
[2] Chu S Z, Inoue S, Wada K, Hishita S and Kumshima K 2005 *Adv. Funct. Mater.* **15** 1343–9
[3] Masuda H, Kanezawa K, Nakao M, Yokoo A, Tamamura T, Sugiura T, Minoura H and Nishio K 2003 *Adv. Mater.* **15** 159–61
[4] Wijnhoven J E G J and Vos W L 1998 *Science* **281** 802–4
[5] Wang X, Meng S, Zhang X, Wang H, Zhong W and Du Q 2007 *Chem. Phys. Lett.* **444** 292–6
[6] Hoyer P 1996 *Langmuir* **12** 1411–3
[7] Cheng L, Zhang X, Liu B, Wang H, Li Y, Huang Y and Du Z 2005 *Nanotechnology* **16** 1341–5
[8] Gong D, Grimes C A, Varghese O K, Hu W, Singh R S, Chen Z and Dickey E C 2001 *J. Mater. Res.* **16** 3331–4
[9] Cai Q, Yang L and Yu Y 2006 *Thin Solid Films* **515** 1802–6
[10] Lockman Z, Ismail S, Sreekantan S, Schmidt-Mende L and MacManus-Driscoll J L 2010 *Nanotechnology* **21** 055601
[11] Paulose M, Shankar K, Yoriya S, Prakasam H E, Varghese O K, Mor G K, Latempa T A, Fitzgerald A and Grimes C A 2006 *J. Phys. Chem.* B **110** 16179–84
[12] Shankar K, Mor G K, Prakasam H E, Yoriya S, Paulose M, Varghese O K and Grimes C A 2007 *Nanotechnology* **18** 065707
[13] Raja K S, Gandhi T and Misra M 2007 *Electrochem. Commun.* **9** 1069–76
[14] Sreekantan S, Hazan R and Lockman Z 2009 *Thin Solid Films* **518** 16–21
[15] Macak J M and Schmuki P 2006 *Electrochim. Acta* **52** 1258–64
[16] Yin H, Liu H and Shen W Z 2010 *Nanotechnology* **21** 035601
[17] Prakasam H E, Shankar K, Paulose M, Varghese O K and Grimes C A 2007 *J. Phys. Chem.* C **111** 7235–41
[18] Daude N, Gout C and Jounin C 1977 *Phys. Rev.* B **15** 3229–35
[19] Liqiang J, Xiaojun S, Weimin C, Zili X, Yauguo D and Honggang F 2003 *J. Phys. Chem. Solids* **64** 615–23
[20] Withana S and Micha T 1982 *J. Electrochem. Soc.* **129** 1240–45
[21] Shi J, Chen J, Feng Z, Chen T, Lian Y, Wang X and Li C 2007 *J. Phys. Chem.* C **111** 693–9
[22] Hu X, Zhang T, Jin Z, Zhang J, Xu W, Yan J, Zhang J, Zhang L and Wu Y 2008 *Mater. Lett.* **62** 4579–81
[23] Zhang Y, Xiao P, Zhou X, Liu D, Garcia B B and Cao G 2009 *J. Mater. Chem.* **19** 948–53
[24] Ren W J, Ai Z H, Jia F L, Zhang L Z, Fan X X and Zou Z G 2007 *Appl. Catal.* B **69** 138–44
[25] Sakthivel S and Kisch H 2003 *Angew. Chem. Int. Edn* **42** 4908–11
[26] Yang X X, Cao C D, Ericksona L, Hohna K, Maghirang R and Klabunde K 2008 *J. Catal.* **260** 126–33
[27] Li Y, Hwang D S, Lee N H and Kim S J 2005 *Chem. Phys. Lett.* **404** 25–9
[28] Gu D E, Lu Y, Yang B C and Hu Y D 2008 *Chem. Commun.* **21** 2453
[29] Wu Z, Dong F, Zhao W, Wang H, Liu Y and Guan B 2009 *Nanotechnology* **20** 235701
[30] Regonini D, Jaroenworaluck A, Stevensa R and Bowena C R 2010 *Surf. Interface Anal.* **42** 139–44
[31] Macak J M, Aldabergerova S, Ghicov A and Schmuki P 2006 *Phys. Status Solidi* a **203** 67–9
[32] Liang H and Li X 2008 *J. Hazard. Mater.* **162** 1415–22
[33] Han X, Kuang Q, Jin M, Xie Z and Zheng L 2009 *J. Am. Chem. Soc.* **131** 3152–3